JBC RESEARCH ARTICLE

Division of labor between the pore-1 loops of the D1 and D2 AAA+ rings coordinates substrate selectivity of the ClpAP protease

Received for publication, August 8, 2021, and in revised form, November 6, 2021 Published, Papers in Press, November 12, 2021,
https://doi.org/10.1016/j.jbc.2021.101407

Kristin L. Zuromski[1], **Sora Kim**[2], **Robert T. Sauer**[2], **and Tania A. Baker**[2,*]

From the [1]*Department of Chemistry, and* [2]*Department of Biology, Massachusetts Institute of Technology, Cambridge, Massachusetts, USA*

Edited by Wolfgang Peti

ClpAP, an ATP-dependent protease consisting of ClpA, a double-ring hexameric unfoldase of the ATPases associated with diverse cellular activities superfamily, and the ClpP peptidase, degrades damaged and unneeded proteins to support cellular proteostasis. ClpA recognizes many protein substrates directly, but it can also be regulated by an adapter, ClpS, that modifies ClpA's substrate profile toward N-degron substrates. Conserved tyrosines in the 12 pore-1 loops lining the central channel of the stacked D1 and D2 rings of ClpA are critical for degradation, but the roles of these residues in individual steps during direct or adapter-mediated degradation are poorly understood. Using engineered ClpA hexamers with zero, three, or six pore-1 loop mutations in each ATPases associated with diverse cellular activities superfamily ring, we found that active D1 pore loops initiate productive engagement of substrates, whereas active D2 pore loops are most important for mediating the robust unfolding of stable native substrates. In complex with ClpS, active D1 pore loops are required to form a high affinity ClpA•ClpS•substrate complex, but D2 pore loops are needed to "tug on" and remodel ClpS to transfer the N-degron substrate to ClpA. Overall, we find that the pore-1 loop tyrosines in D1 are critical for direct substrate engagement, whereas ClpS-mediated substrate delivery requires unique contributions from both the D1 and D2 pore loops. In conclusion, our study illustrates how pore loop engagement, substrate capture, and powering of the unfolding/translocation steps are distributed between the two rings of ClpA, illuminating new mechanistic features that may be common to double-ring protein unfolding machines.

ATPases associated with diverse cellular activities (AAA+) superfamily enzymes perform energy-dependent macromolecular remodeling required for protein degradation, DNA replication and repair, organelle biogenesis, and membrane fusion within the cells of all organisms (1–3). Protein degradation by AAA+ proteases is important for maintaining protein homeostasis by eliminating damaged or unneeded proteins, recycling amino acids, and regulating the proteome in response to environmental stressors (4, 5). The *Escherichia coli* ClpAP quality-control protease is an assembly of the double-ring AAA+ $ClpA_6$ unfoldase/translocase and the $ClpP_{14}$ peptidase (6, 7). In collaboration with its adapter protein ClpS, ClpAP degrades N-end rule (N-degron) pathway substrates (8–10).

ClpA has two AAA+ rings, termed D1 and D2, that stack within the hexamer. Although each ring contains six ATP-hydrolysis modules, the D1 and D2 ATPase sites contribute differentially to unfolding and degradation. D2 is the more robust ATPase and can unfold and translocate many protein substrates when ATP hydrolysis in D1 is inactivated, whereas ATP hydrolysis in D1 is important for degradation processivity and for assisting D2 in unfolding very stable native substrates (11–13). Pore-1 loops (hereafter called pore loops) line the central channel of the D1 and D2 rings. Each pore loop contains a conserved tyrosine side chain that contacts peptide segments of substrates within the pore channel and is implicated in the substrate binding, unfolding, and translocating steps required for degradation (14–16) (Fig. 1*A*). The D1 and D2 pore loops have distinct sequences and conservation patterns. "GYVG"-family pore loops are found in the D2 rings of many double-ring unfoldases, as well as in single-ring unfoldases, whereas "KYR"-family pore loops are found in the D1 modules of ClpA and many other double-ring protein degradation and/or remodeling machines (15, 17–19) (Fig. 1*A*). Tyrosine to alanine mutations in either the D1 ring (Y259A) or D2 ring of ClpA (Y540A) eliminate or hinder ClpAP degradation of all substrates tested (15, 20, 21). These severe defects have made it difficult to determine the unique roles and possible coordination between pore loops in the D1 and D2 rings; elucidating these specific roles is critical for understanding the molecular mechanisms used by ClpA and related double-ring unfoldases.

ClpA recognizes degrons (degradation tags) of substrates either directly or indirectly *via* delivery by the ClpS adapter. During direct recognition, the ClpA pore physically binds the unstructured degron peptide. For example, the ssrA degron (AANDENYALAA-COOH) is cotranslationally

* For correspondence: Tania A. Baker, tabaker@mit.edu.
Present address for Kristin L. Zuromski: Kymera Therapeutics, Watertown, Massachusetts 02472, USA.

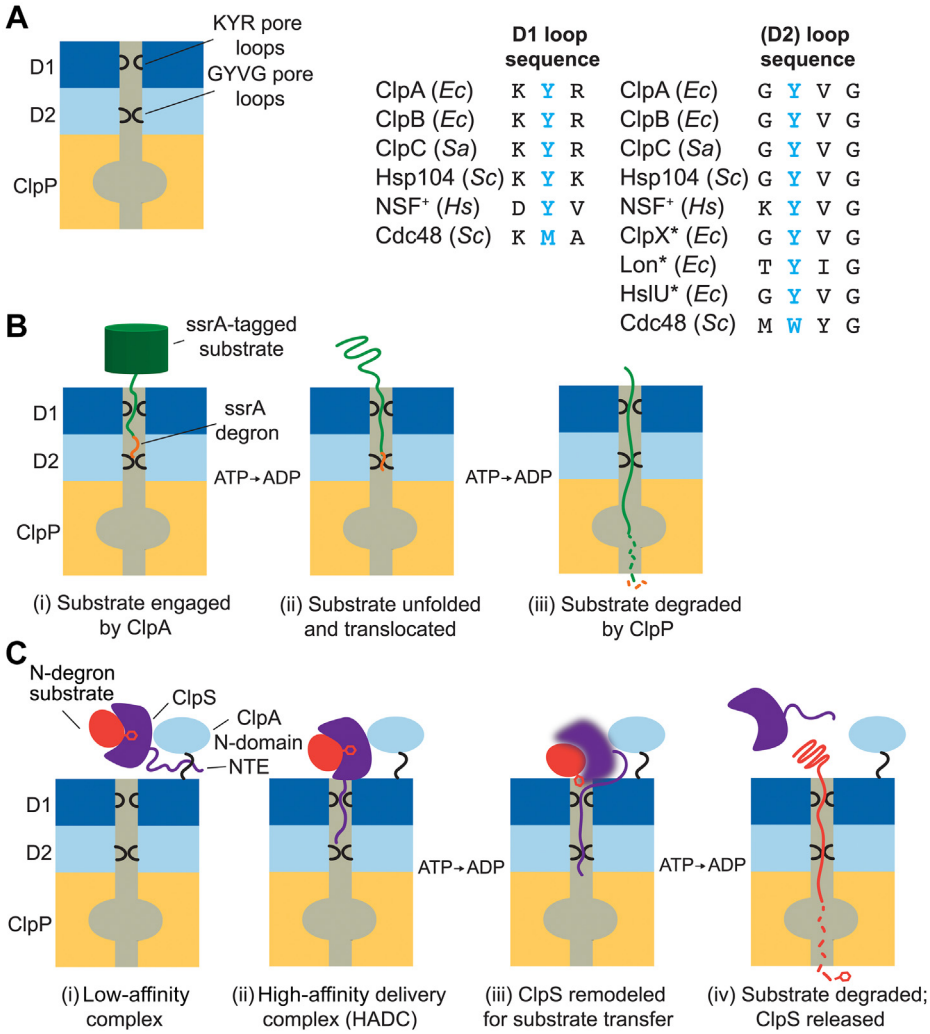

Figure 1. Substrate degradation by ClpAP. *A*, *left*, diagram of the two sets of pore-1 loops in ClpA. The D1 ring pore loops contain the "KYR" motif, whereas the D2 rings contain a "GYVG" motif. *Right*, alignment of ClpA pore-1 loops with those of other double or single (*) ring AAA+ unfoldases. Single-ring unfoldases carry the "GYVG" motif in their one AAA+ ring, which aligns best with the D2 rings of many double-ring enzymes. In the double-ring enzyme NSF (+), the pore-loop motifs are reversed between the rings, with D1 containing the "GYVG" sequence and the D2 containing a sequence more similar to "KYR". *B*, degradation of substrates with an ssrA degron (*red*) by ClpAP. ClpA (*blue*) uses ATP hydrolysis to (i) bind/engage, (ii) unfold/translocate an ssrA-tagged substrate (*green*) into the ClpP peptidase (*yellow*) for (iii) degradation. *C*, ClpS-mediated degradation of an N-degron substrate. ClpS (*purple*) bound to an N-degron substrate (*red*) is (i) engaged by ClpA's N-domain (*blue oval*; only one of six is shown for clarity), forming a low-affinity complex; (ii) additional contacts between ClpS's core domain, N-terminal extension (NTE) (*purple line*), and N-degron substrate with ClpA's D1 domain (*dark blue*, *top*) form a high-affinity delivery complex (HADC); (iii) ATP-dependent remodeling of ClpS brings the substrate closer to the ClpA pore, allowing for (iv) ClpAP-mediated degradation of the substrate and proposed release of ClpS from ClpA. AAA+, ATPases associated with diverse cellular activities; *Ec*, *Escherichia coli*; *Hs*, *Homo sapiens*; *Sa*, *Staphylococcus aureus*; *Sc*, *Saccharomyces cerevisiae*.

appended to proteins translated from mRNAs lacking a stop codon, as well as during other types of translational stress, and targets the tagged protein for degradation by multiple proteases, including ClpAP (22, 23). The ssrA degron has been extensively used in biochemical experiments and is sufficient to target essentially any protein for ClpAP degradation (15, 24, 25). After binding the ssrA tag of a substrate, ATP hydrolysis by ClpA powers engagement, unfolding, and translocation of the substrate through ClpA's axial channel and into the protease chamber of ClpP for degradation (5, 26) (Fig. 1*B*).

The substrate specificity of ClpA is modified by the ClpS adapter, which binds and delivers substrates with N-degrons for degradation within the ClpAPS complex (8–10). ClpS also inhibits ClpAP recognition and the subsequent degradation of ssrA-tagged proteins and other directly recognized substrates by weakening their affinity for ClpA and reducing ClpA's ATPase rate; this suppression of ATP-hydrolysis by ClpS slows protein degradation by ClpAP (8, 27–29). This mechanism ensures that ClpAPS has a very strong preference for degrading N-degron substrates and illustrates how an adapter can modify both an enzyme's catalytic activity and substrate specificity. In *E. coli*, ClpAPS efficiently degrades proteins bearing N-terminal Phe, Leu, Trp, or Tyr residues (8, 10, 30). ClpS has an intrinsically disordered N-terminal extension (NTE; residues 2–25) and a folded core domain (residues 26–106). The ClpS core contains a binding pocket for N-degrons and a binding surface for the N-domain of ClpA

(31, 32). ClpS bound to an N-degron substrate initially forms a low-affinity complex with one of the N-domains of ClpA, but upon ATP-dependent engagement of the ClpS NTE within the ClpA channel, a high-affinity delivery complex (HADC) is formed (33, 34) (Fig. 1*C*). Key contacts within these delivery complexes include interactions between: (i) ClpS and the N-degron substrate; (ii) ClpS and the ClpA N-domain; and (iii) the ClpS NTE and the ClpA pore. In the HADC, the NTE in the ClpA channel is proposed to serve as a "degron mimic". By a current model, ClpA is thought to engage and "tug" on the NTE; this mechanical force alters the conformation of ClpS, bringing the N-degron substrate to the ClpA pore and perhaps releasing ClpS (33, 34) (Fig. 1*C*). Although substantial evidence supports the idea that N-degron delivery from the HADC to the ClpA channel requires ATP hydrolysis by ClpA, the mechanistic details of this key step are uncertain and relatively little is known about how ClpA remodels the ClpS•substrate complex to allow transfer of the N-degron from ClpS to the ClpAP channel for degradation (27, 33, 34).

Here, we elucidate the roles of the ClpA D1 and D2 pore loops during substrate unfolding, polypeptide translocation, and ClpS remodeling. Using targeted mutagenesis coupled with protein crosslinking to assemble specific configurations of ClpA with different numbers and arrangements of mutant pore loops, we identify the contributions of pore loops to direct engagement, unfolding, and translocation of a set of ssrA-tagged substrates with different folding characteristics. Likewise, we use the ClpA pore-loop variants to parse the mechanical contributions of ClpA among the steps in ClpS-initiated degradation of N-degron substrates. We find that the D1 pore loops are important for initially capturing substrates and contribute to translocation, particularly for unfolded substrates, whereas the D2 pore loops are required for unfolding and translocating native substrates. We also show that the ClpS NTE interacts in a distinct manner with the D1 *versus* the D2 pore loops. Overall, our results reveal that ClpA uses a similar mechanism to remodel ClpS as it does to unfold and translocate ssrA-tagged substrates. Taken together, these observations contribute to our understanding of the mechanisms for coordinated work by individual components of the double-ring unfoldases.

Results

Assembly of ClpA with different numbers of WT pore loops

We previously used a cysteine crosslinking strategy to covalently link two ClpA subunits and thereby enable specific mutations to be introduced into three or six ClpA protomers in an assembled hexamer (12) (Fig. 2*A*). Using an otherwise cysteine-free background, we introduced either the D645C or Q709C substitution into ClpA monomers to promote a specific, covalent crosslink between two neighboring subunits in the final hexamer. These ClpA crosslinking variants also carried the ΔC9 deletion, which removes ClpA's intrinsic degradation signal to prevent auto-degradation of ClpA by ClpAP (35). A mutation of either the conserved D1 or D2 pore-1-loop tyrosine (Y259A or Y540A, respectively) was also introduced into either one or both crosslinkable ClpA monomers. We then generated a group of pseudohexamers by mixing equal amounts of two ClpA-crosslinking variants with the desired pore-loop mutations, followed by covalent crosslinking and ATP-dependent assembly of trimers of crosslinked dimers (12) (Fig. 2*B*).

ClpA pseudohexamers were constructed with different arrangements of pore loops: (i) all WT pore loops ($ClpA^{xl}$); (ii) alternating WT and defective D1 pore loops ($^{D1\text{-}3YA}ClpA^{xl}$); (iii) six defective D1 pore loops ($^{D1\text{-}6A}ClpA^{xl}$); (iv) alternating WT and defective D2 pore loops ($^{D2\text{-}3YA}ClpA^{xl}$); and (v) six defective D2 pore loops ($^{D2\text{-}6A}ClpA^{xl}$) (Fig. 2*B*). All variants stimulated the cleavage of a fluorescent decapeptide in an assay that requires ClpA to dock with ClpP but does not depend on protein unfolding or translocation (12, 36) (Fig. 2*C*), demonstrating that neither the crosslinking nor the pore-loop mutations interfered with the ability of ClpA to form active complexes with ClpP.

We used our crosslinked ClpA variants with different combinations of WT and defective D1 or D2 pore loops to probe the roles of these loops in specific stages of the ClpAP degradation cycle. First, we investigated ssrA degron engagement and analyzed how specific pore loops function in mechanical unfolding and translocation. Next, we used a similar approach to dissect how the different pore loops contribute to the multiple steps of N-degron substrate delivery to ClpAP by ClpS.

D1 pore loops engage and translocate ssrA substrates

We examined how mutation of the D1 or D2 pore loops affects ClpAP degradation of an ssrA-tagged titin^{I27} domain unfolded by chemical modification of its two partially buried cysteines (^{UF}titin-ssrA) (37, 38). Degradation of this substrate requires specific recognition by ClpA and translocation into ClpP but does not require enzymatic unfolding. Importantly, translocation and degradation of this substrate required ATP hydrolysis by ClpA, as proteolysis did not occur in control reactions containing ATPγS (which is not detectably hydrolyzed by ClpA) (Fig. S1). $^{D1\text{-}3YA}ClpA^{xl}$, $^{D2\text{-}3YA}ClpA^{xl}$, and $^{D2\text{-}6A}ClpA^{xl}$ degraded ^{UF}titin-ssrA at rates similar to, or faster than, $ClpA^{xl}$ (Fig. 3*A*, compare variants 2, 4, and 5 to variant 1). In contrast, $^{D1\text{-}6A}ClpA^{xl}$ was severely defective at degrading this substrate (Fig. 3*A*, variant 3). Thus, the WT D1, but not the D2 pore loops, is needed for efficient ^{UF}titin-ssrA degradation. The degradation defect of $^{D1\text{-}6A}ClpA^{xl}$ was partially overcome by increasing concentrations of ^{UF}titin-ssrA (Fig. 3*B*, variant 3); however, these data could not reliably be fit to the Michaelis–Menten equation to determine K_M and V_{max} values. To calculate an estimate for the K_M, we assumed that this variant's V_{max} was similar to that of $ClpA^{xl}$; this assumption allowed us to estimate that the K_M for the ^{UF}titin-ssrA substrate would be at least 40-fold weaker for $^{D1\text{-}6A}ClpA^{xl}$ than for the parental enzyme (Table S1). In contrast, the variant with three WT D1 pore loops ($^{D1\text{-}3YA}ClpA^{xl}$) degraded ^{UF}titin-ssrA

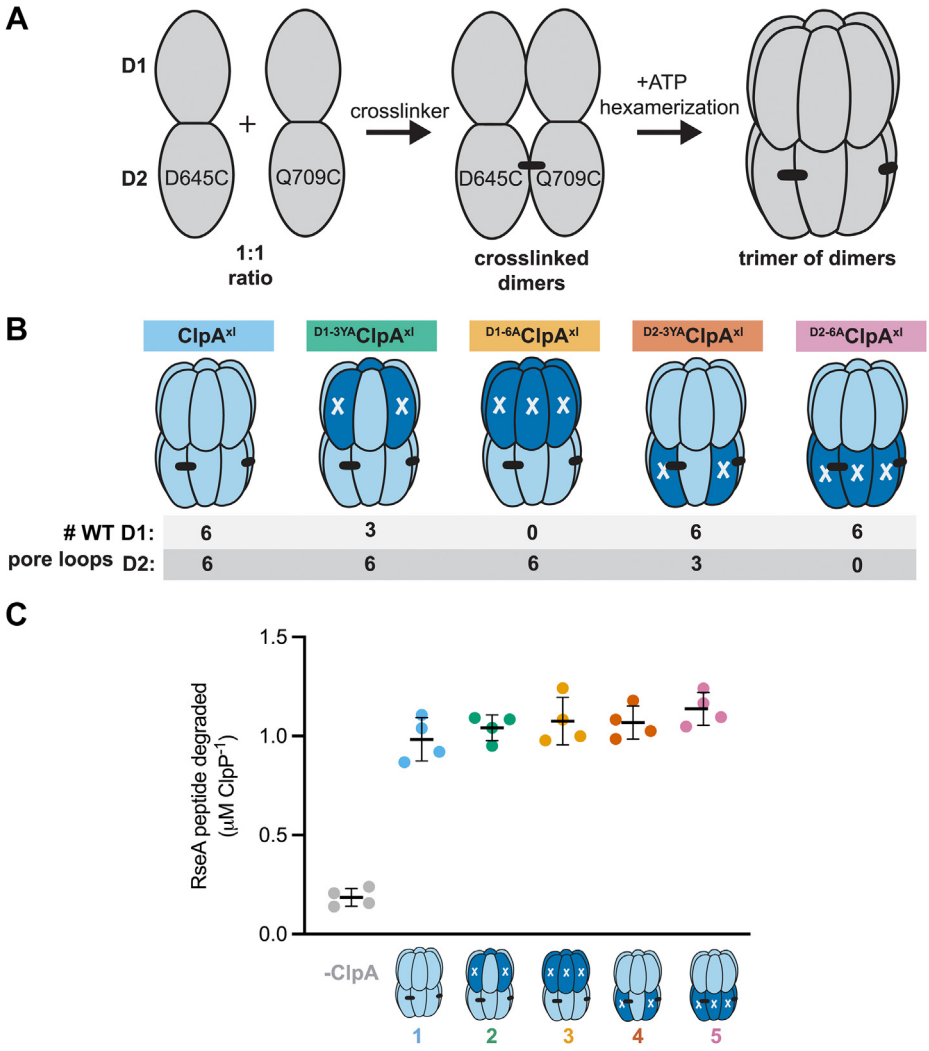

Figure 2. Assembly of ClpA variants with different arrangements of mutant pore loops. *A*, schematic of ClpA subunit crosslinking using engineered D645C or Q709C crosslinking sites in the ClpA D2 module. The addition of a homobifunctional crosslinker generates crosslinked dimers containing the two classes of protomers, which are then assembled into pseudohexamers with ATP. *B*, cartoons of ClpA D1 (Y259A) or D2 (Y540A) pore-loop substitutions with the hexameric arrangements used in this study; modules in *dark blue* with a white "X" carry the defective pore-loop mutation. The names of each variant and their corresponding colors used in figures are above each cartoon. *C*, ClpA variants interact with ClpP as assayed by a pore-opening assay. $ClpP_{14}$ (0.25 μM) cleavage of a fluorogenic RseA decapeptide (15 μM) was assayed in the presence of each of the ClpA variants (0.5 μM $ClpA_6$) and ATPγS (2 mM). *Gray symbols* show the activity of the ClpP-only "no ClpA" control. The summary data are averages (n ≥ 3) ± 1 SD.

substantially faster than $^{D1\text{-}6A}ClpA^{xl}$ (Fig. 3*B*, compare variant 2 to variant 3). $^{D1\text{-}3YA}ClpA^{xl}$ degraded ^{UF}titin-ssrA with a V_{max} similar to $ClpA^{xl}$, indicating that the two enzymes have comparable translocation activity. However, $^{D1\text{-}3YA}ClpA^{xl}$ degraded this substrate with a three-fold weaker K_M than $ClpA^{xl}$, demonstrating a modest defect in substrate binding/engagement (Table S1). Together, these results support the conclusion that the WT D1 pore loops are required for efficient recognition and productive engagement of ssrA-tagged substrates. The concentration dependence of degradation also revealed that variants with zero or three WT D2 pore loops had K_M values similar to the $ClpA^{xl}$ control but had higher V_{max} values (Fig. 3*B*, compare variants 4 and 5 to variant 1; Table S1). Thus, in contrast to the D1 pore loops, WT D2 pore loops are not needed for efficient engagement of ^{UF}titin-ssrA and in fact slow degradation, likely by slowing translocation in some fashion (see Discussion).

D2 and D1 pore loops are needed for substrate unfolding

We next tested ClpAP-mediated degradation of a natively folded substrate, $titin^{V13P}$-ssrA, which is less thermodynamically stable and degraded more rapidly by ClpAP than the parental $titin^{I27}$-ssrA substrate (39). $^{D1\text{-}6A}ClpA^{xl}$ failed to degrade $titin^{V13P}$-ssrA, as expected based on the recognition defect described above, but $^{D2\text{-}6A}ClpA^{xl}$ was also inactive, supporting a role for WT D2 loops in unfolding $titin^{V13P}$-ssrA (Fig. 3*C*). Interestingly, $ClpA^{xl}$ and $^{D2\text{-}3YA}ClpA^{xl}$ degraded $titin^{V13P}$-ssrA at comparable rates, whereas $^{D1\text{-}3YA}ClpA^{xl}$ was inactive (Fig. 3*C*). Thus, a subset of WT D2 pore loops is

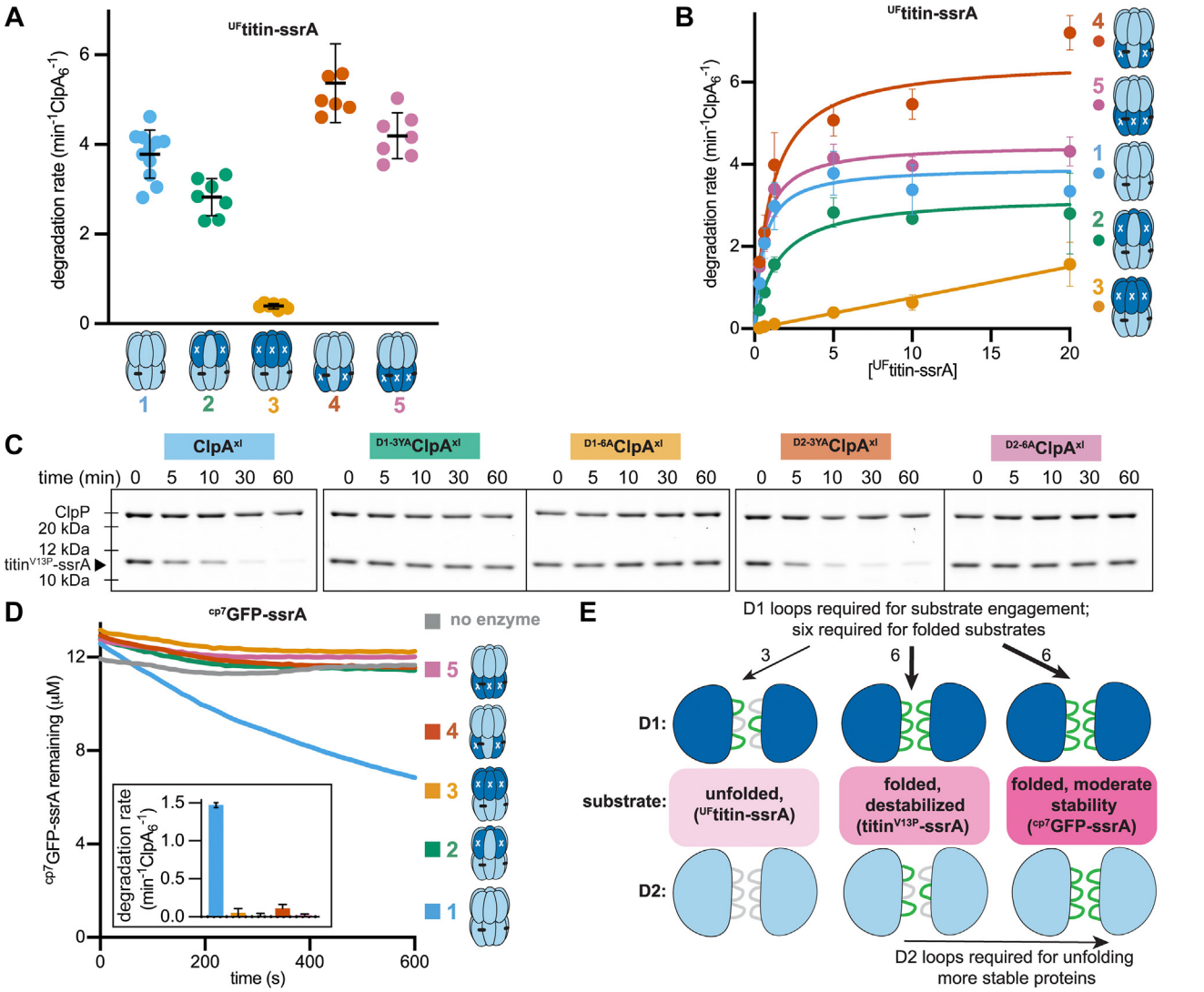

Figure 3. Degradation of ssrA degron substrates with ClpA pore-loop variants. *A*, rates of ^{UF}titin-ssrA (5 μM) degradation by ClpA pore-loop variants with ClpP (0.1 μM $ClpA_6$, 0.3 μM $ClpP_{14}$) and ATP (4 mM). The summary data are means ±1 SD (n ≥ 7). *B*, Michaelis–Menten analysis of ^{UF}titin-ssrA degradation kinetics by ClpAP pore-loop variants. See Table S1 for values. *C*, representative SDS-PAGE showing degradation of titin^{V13P}-ssrA (10 μM, *black arrow*) by ClpAP variants (0.25 μM $ClpA_6$, 0.75 μM $ClpP_{14}$) with ATP (5 mM). *D*, representative degradation kinetics of ^{cp7}GFP-ssrA (10 μM) by ClpAP (0.3 μM $ClpA_6$, 0.8 μM $ClpP_{14}$) with ATP (4 mM). The *inset* shows the quantified degradation rates. The summary data are means ±1 SD (n = 3). *E*, cartoon summary of the number of D1 and D2 pore loops required to degrade ssrA-tagged substrates, with the stabilities of the substrates increasing from *left* to *right* across the panel. WT pore loops are in *green* and the defective pore loops are in *gray*.

sufficient to unfold titin^{V13P}-ssrA, whereas a full complement of WT D1 loops appears to be required to form a productive enzyme•substrate complex with this natively folded ssrA-tagged protein.

Then, we tested ClpAP degradation of ^{cp7}GFP-ssrA, a natively folded, circularly-permuted variant of GFP (40). This substrate was degraded poorly by all the pore-loop variants, with kinetic traces resembling the "no enzyme" control (Fig. 3*D*). Although we could ascribe the $^{D1\text{-}6A}$ClpA^{xl} defect to impaired substrate recognition, the meager activity of the remaining pore-loop variants further suggested that a full complement of both the WT D1 and D2 pore loops is required for engagement, unfolding, and degradation of this stable, natively folded substrate.

Overall, our degradation results with ^{UF}titin-ssrA, titin^{V13P}-ssrA, and ^{cp7}GFP-ssrA establish that the D1 pore loops play major roles in recognition and translocation of ssrA-tagged substrates, whereas the D2 loops are key participants in native substrate unfolding but also require assistance from the D1 pore loops to process increasingly stable substrates (Fig. 3*E*). Because unfolding is thought to occur by the same power-stroke mechanism as translocation, the D2 pore loops also likely assist in translocation, as we demonstrate below.

D1 and D2 pore loops are critical in ClpAPS-promoted degradation

The NTE of ClpS is proposed to be engaged by ClpA and act as a "degron mimic", meaning that it is bound and "pulled on" by functional groups in the enzyme's central channel (33, 34). However, the NTE is not a true degron in the context

of ClpS because ClpS is not degraded by ClpAP (29, 33). To understand the roles of the different pore loops during ClpS delivery of N-degron substrates, we investigated the requirements for D1 and D2 pore loops during ClpAPS-complex formation and degradation of N-end rule substrates. Using our pore-loop variants, we initially tested ClpAPS degradation of YLFVQELA-GFP, a natively folded N-degron substrate (27, 33, 34, 41). The mutation of three or six D1 or D2 pore loops dramatically reduced the rates of YLFVQELA-GFP degradation compared with those observed with the parental $ClpA^{xl}$ enzyme (Fig. 4*A*). Although these results highlight important roles for the D1 and D2 pore loops in ClpAPS-promoted degradation, the absence of appreciable activity precluded dissection of their specific functions.

Next, we assayed ClpAPS degradation of ^{UF}YLFVQ-titin, an unfolded N-degron substrate (28, 34, 38, 41). $ClpA^{xl}$, $^{D1\text{-}3YA}ClpA^{xl}$, and $^{D2\text{-}3YA}ClpA^{xl}$, all promoted substantial levels of ClpS-dependent degradation of ^{UF}YLFVQ-titin (Fig. 4*B*, yellow symbols, compare variants 1,2, and 4). Thus, three WT D1 pore loops in the context of a fully active D2 ring or three WT D2 pore loops in the context of a fully active D1 ring are sufficient for ClpAPS degradation of this N-degron substrate.

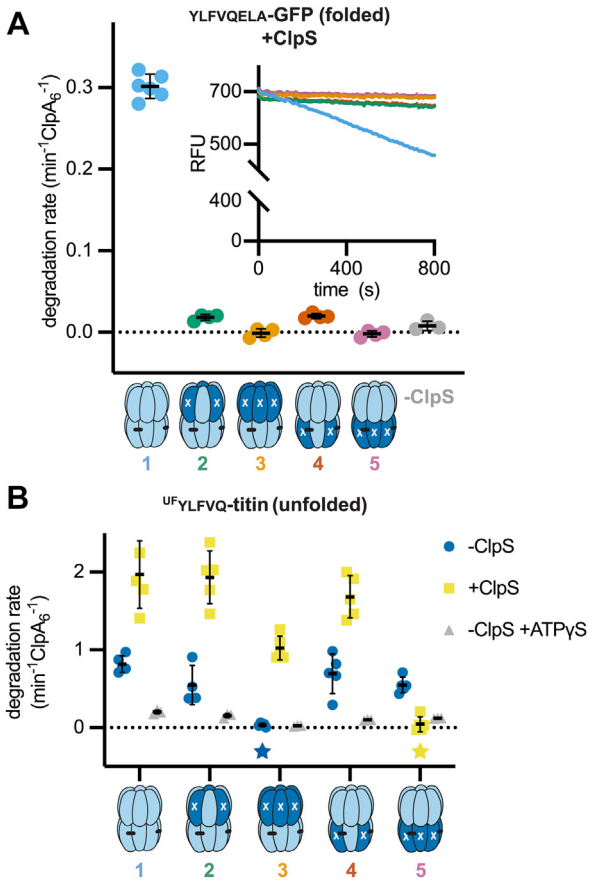

Figure 4. D1 and D2 pore loops are required for the degradation of N-degron substrates. *A*, degradation rates of YLFVQELA-GFP (1 μM) by ClpAPS pore-loop variants (0.1 μM $ClpA_6$, 0.3 μM $ClpP_{14}$, 1 μM ClpS) and ATP (4 mM). The final points (*gray*) are for the $ClpA^{xl}$ WT control without ClpS. The summary data are means ±1 SD (n = 4). The *inset* shows representative kinetic traces. *B*, degradation rates of ^{UF}YLFVQ-titin (1 μM) by ClpA variants (0.1 μM $ClpA_6$, 0.3 μM $ClpP_{14}$,) with ATP (4 mM) in the absence (*blue circles*) or presence (*yellow squares*) of ClpS (1.0 μM) or with ATPγS (2 mM) in the absence of ClpS (*gray triangles*). The summary data are means ±1 SD (n ≥ 3).

Two pore-loop variants displayed behaviors that provided additional functional insights. First, $^{D1\text{-}6A}ClpA^{xl}$, with no WT D1 pore loops, degraded ^{UF}YLFVQ-titin in the presence, but not the absence, of ClpS (Fig. 4*B*, marked by the blue star, variant 3: compare blue to the yellow symbol clusters). This positive degradation activity with ClpS demonstrates that although WT D1 pore loops can contribute to translocation of unfolded and folded ssrA-tagged substrates (Fig. 3), they are not required for translocation of an unfolded N-degron substrate. In the absence of ClpS, the $^{D1\text{-}6A}ClpA^{xl}$ variant cannot degrade the substrate, consistent with the recognition/engagement defect observed previously during direct recognition of ssrA-tagged substrates (Fig. 3, *A* and *B*). Importantly, the ability of ClpS to activate $^{D1\text{-}6A}ClpA^{xl}$-supported degradation of ^{UF}YLFVQ-titin indicates that WT D1 pore loops play different roles in direct recognition of ssrA-tagged substrates than during ClpS-mediated substrate recognition, at least with the unfolded protein substrates we tested.

Second, $^{D2\text{-}6A}ClpA^{xl}$, with no WT D2 pore loops, degraded ^{UF}YLFVQ-titin in the absence, but not the presence, of ClpS (Fig. 4*B* yellow star, variant 5; compare blue to yellow symbols). Without ClpS, $^{D2\text{-}6A}ClpA^{xl}$ performed degradation at a rate only slightly slower than the parental enzyme (Fig. 4*B*, compare variant 5 to variant 1; blue symbols), consistent with the substrate being unfolded and therefore not requiring the unfolding activity of the D2 ring. In marked contrast, however, $^{D2\text{-}6A}ClpA^{xl}$ failed to degrade ^{UF}YLFVQ-titin in the presence of ClpS (Fig. 4*B*, variant 5; yellow symbols). These data strongly suggest that the D2 ring has a very important role during ClpS-dependent degradation of N-degron substrates, and that this activity is distinct from substrate unfolding. These results prompted us to investigate D1 and D2 pore-loop functions during ClpS-mediated substrate delivery in greater detail.

ClpA D1 pore loops mediate interactions with ClpS and N-degron substrates

Formation of a HADC containing ClpAP, ClpS, and an N-degron substrate is required for N-degron substrate degradation (33, 34). To assess the roles of the D1 and D2 pore loops in HADC formation, we probed reactions containing our set of D1 and D2 pore-loop variants using assays that monitored assembly and/or protein-protein interactions, rather than degradation. To detect ternary-complex assembly between ClpA, ClpS, and substrate, we titrated an equimolar mixture of $ClpA_6$ and ClpS against a fixed concentration of a fluorescent N-degron peptide (LLYVQRDSKEC-fl) and monitored assembly by increases in fluorescence anisotropy (Fig. 5*A*). Both $ClpA^{xl}$ and $^{D2\text{-}6A}ClpA^{xl}$ formed ternary complexes with ClpS and the N-degron peptide with similar apparent affinities (K_{app}) of 0.18 ± 0.01 μM and 0.25 ± 0.01 μM, respectively. The omission of ClpA or ClpS resulted in no detectable ternary-complex formation (Fig. 5*A*, unfilled symbols). Thus, WT D2 pore loops are not required for a high-affinity interaction between ClpA, ClpS, and the N-degron peptide. In contrast, the

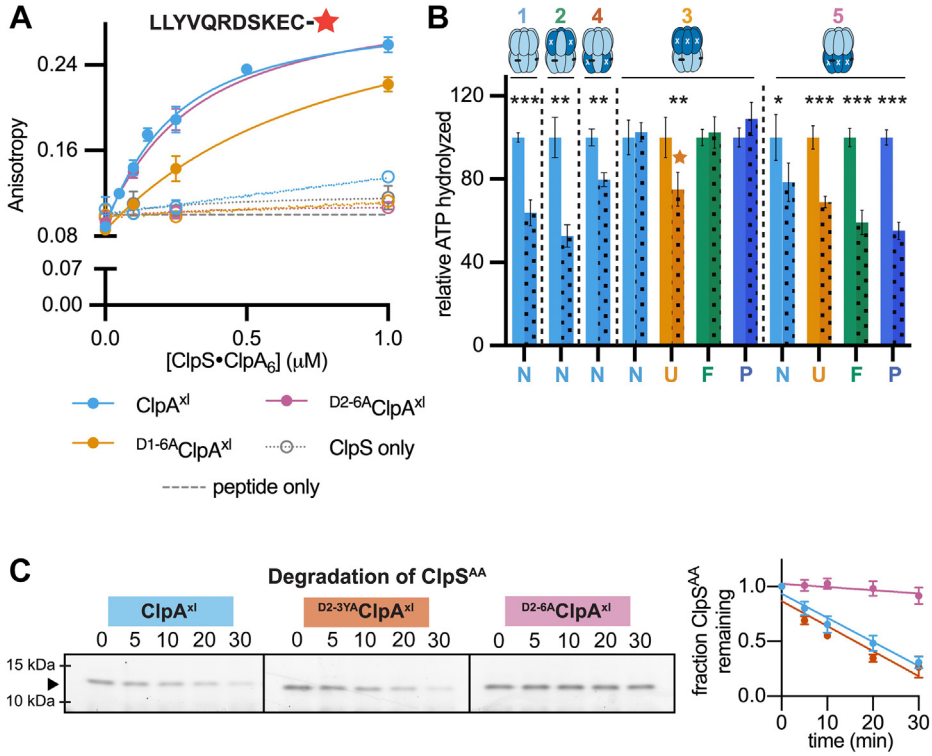

Figure 5. D1 pore loops mediate interactions with ClpS and substrate. *A*, increasing concentrations of an equimolar mixture of $ClpA_6$ and ClpS were titrated against a fixed concentration LLYVQRDSKEC-fl (100 nM) in the presence of ATPγS (2 mM). *Solid colored lines* are fluorescence anisotropy values of ClpA pore-loop variants plus ClpS and corresponding *dotted lines* with *unfilled circles* are "ClpA only" controls (no ClpS plus 2 mM ATPγS). ClpS only (*gray dotted line*, *unfilled circles*) and peptide only (*dashed gray line*) data are also shown. As noted previously, ClpA with all of its natural cysteine residues removed has modestly lower activity than the WT, and cysteine crosslinking also slightly lowers ClpA activity in some assays (12); we attribute the weaker binding of the ClpS–peptide complexes to the ClpA variants used here than the binding observed with uncrosslinked, WT ClpA to these effects (33). *B*, relative rate of ATP hydrolysis of 5 mM ATP by ClpAP variants (0.1 μM $ClpA_6$, 0.3 μM $ClpP_{14}$) in the absence (*solid bars*) or presence (*patterned bars*) of ClpS (1 μM), measured with no substrate (*light-blue bars*, N), unfolded ^{UF}YLFVQ-titin (1 μM, *orange bars*, U), folded YLFVQELA-GFP (1 μM, *green bars*, F), or LLYVQRDSKEC-amide peptide (20 μM, *dark-blue bars*, P). For each condition, the rates are relative to the rate without ClpS or substrate, which was set to 1. The summary data are means ±1 SD (n ≥ 3). +ClpS data were compared with -ClpS data by an unpaired *t* test (***$p \le 0.001$; **$p \le 0.01$; *$p \le 0.05$). *C*, *left*, representative SDS-PAGE degradation reactions of $ClpS^{AA}$ ($ClpS^{P24A,P25A}$, 5 μM) by ClpA pore-loop variants (0.25 μM $ClpA_6$, 0.75 μM $ClpP_{14}$) and ATP (5 mM). *Right*, quantification of $ClpS^{AA}$ remaining, with each point representing the means of observed values in independent experiments ±1 SD (n ≥ 3).

K_{app} for binding by $^{D1\text{-}6A}$ClpA^{xl} was weaker at 0.76 ± 0.03 μM (Fig. 5*A*), showing that ClpA without WT D1 pore loops formed a less stable ternary complex. These results therefore support the conclusion that WT D1 pore loops (but not D2 loops) participate in assembly of stable HADCs.

ClpS binding to ClpA inhibits degradation of the ssrA-tagged substrates in part by suppressing the ATPase activity of ClpA ~2-fold (27, 28). Thus, we used ATPase suppression as an assay for assembly of functional ClpAPS complexes using the panel of pore-loop-defective ClpA variants. ClpS reduced the ATPase activities of the ClpA^{xl} control, $^{D1\text{-}3YA}$ClpA^{xl}, $^{D2\text{-}3YA}$ClpA^{xl}, and $^{D2\text{-}6A}$ClpA^{xl} by ~25 to 50% (Fig. 5*B*; variants 1, 2, 4, 5; N (no substrate); light blue bars; solid bars = no ClpS, patterned bars = +ClpS). In marked contrast, ClpS did not suppress ATP hydrolysis by $^{D1\text{-}6A}$ClpA^{xl} (variant 3; N; light blue bars). Thus, based on the ATPase suppression, we conclude that some WT D1 pore loops are important in forming optimal ClpAPS complexes, in agreement with the fluorescence anisotropy experiment (Fig. 5*A*). We also tested ClpS-dependent ATPase suppression in the presence of unstructured or native N-degron substrates. ClpS reduced ATP hydrolysis by $^{D2\text{-}6A}$ClpA^{xl} in the presence of (i) an N-degron peptide (LLYVQRDSKEC-amide; P), (ii) unfolded ^{UF}YLFVQ-titin (U), and (iii) folded YLFVQELA-GFP (F) (Fig. 5*B*; variant 5; dark blue, orange, green bars, respectively), reinforcing the conclusion that WT D2 pore loops are not essential for assembly of functional ClpA•ClpS complexes. In contrast, ClpS did not suppress ATP hydrolysis by $^{D1\text{-}6A}$ClpA^{xl} in the presence of either the peptide substrate or YLFVQELA-GFP (Fig. 5*B*; variant 3; dark blue and green bars). Thus, based on fluorescence anisotropy assembly experiments and measuring ClpS-dependent suppression of ClpA's ATPase rate, we conclude that the D1 pore loops, but not those in the D2 ring, are important for the assembly of ClpS•ClpA complexes.

However, one surprising observation suggested that the role of D1 pore loops in assembly of complexes is likely multifaceted and can depend on features of the substrate: we observed that in the presence of the long, chemically unfolded N-degron substrate, ^{UF}YLFVQ-titin, ClpS-suppressed ATP hydrolysis by $^{D1\text{-}6A}$ClpA^{xl} to about half the extent observed with the ClpA^{xl} control (Fig. 5*B*; variant 3, orange bars, compare to variant 1, light blue bars). These data indicate that some functional ClpS•ClpAP•substrate complexes form under these conditions. This ATPase suppression result paralleled the partial

degradation of ^{UF}YLFVQ-titin by $^{D1\text{-}6A}$ClpA^{xl}PS observed above (Fig. 4*B*, variant 3), which also was the only tested substrate that $^{D1\text{-}6A}$ClpA^{xl} could degrade at a detectable level. These results indicate that the important role D1 pore loops contribute to assembly of functional ClpS•ClpAP•N-degron-substrate HADC complexes can be partially bypassed depending on the specific characteristics of the substrate.

D2 pore loops are required for ClpS remodeling

ClpA is thought to catalyze ATP-hydrolysis-dependent remodeling of the ClpS-core structure during N-degron substrate delivery (27, 33, 34). Although $^{D2\text{-}6A}$ClpA^{xl}, which lacks WT D2 pore loops, forms high-affinity complexes with ClpS and N-degron substrates (Fig. 5*A*), this mutant supported ClpAPS degradation of ^{UF}YLFVQ-titin very poorly, with a rate ~100-fold slower than that of the parental enzyme (Fig. 4*B*). These data suggest that the critical ClpS-remodeling step, which occurs after HADC formation but before degradation, is likely mediated by the pore loops of the D2 ring.

To test this hypothesis further, we used a mutant variant of ClpS in which the mechanical activity ClpA exerts on the adapter could be observed directly. Recall that ClpS is composed of a 25-residue, poorly structured NTE followed by a tightly folded core domain (residues 26–106) that contains both the binding sites for the ClpA N-domain and the N-degron (Fig. S2*A*). The NTE contains a stretch of ~5 residues adjacent to the ClpS core called the junction sequence. The junction sequence is moderately conserved among bacterial ClpS orthologs in contrast to the rest of the NTE, which shows little sequence conservation (33, 42). A hallmark of the junction sequence is that it contains 1 to 3 prolines; the *E. coli* ClpS NTE carries residues Pro^{24} and Pro^{25} (Fig. S2*A*). WT ClpS is not degraded by ClpAP (29, 33), whereas changing these two prolines to alanines (to make ClpS^{AA}) renders ClpS susceptible to degradation (Fig. 5*C*) (42). Thus, in addition to the stable

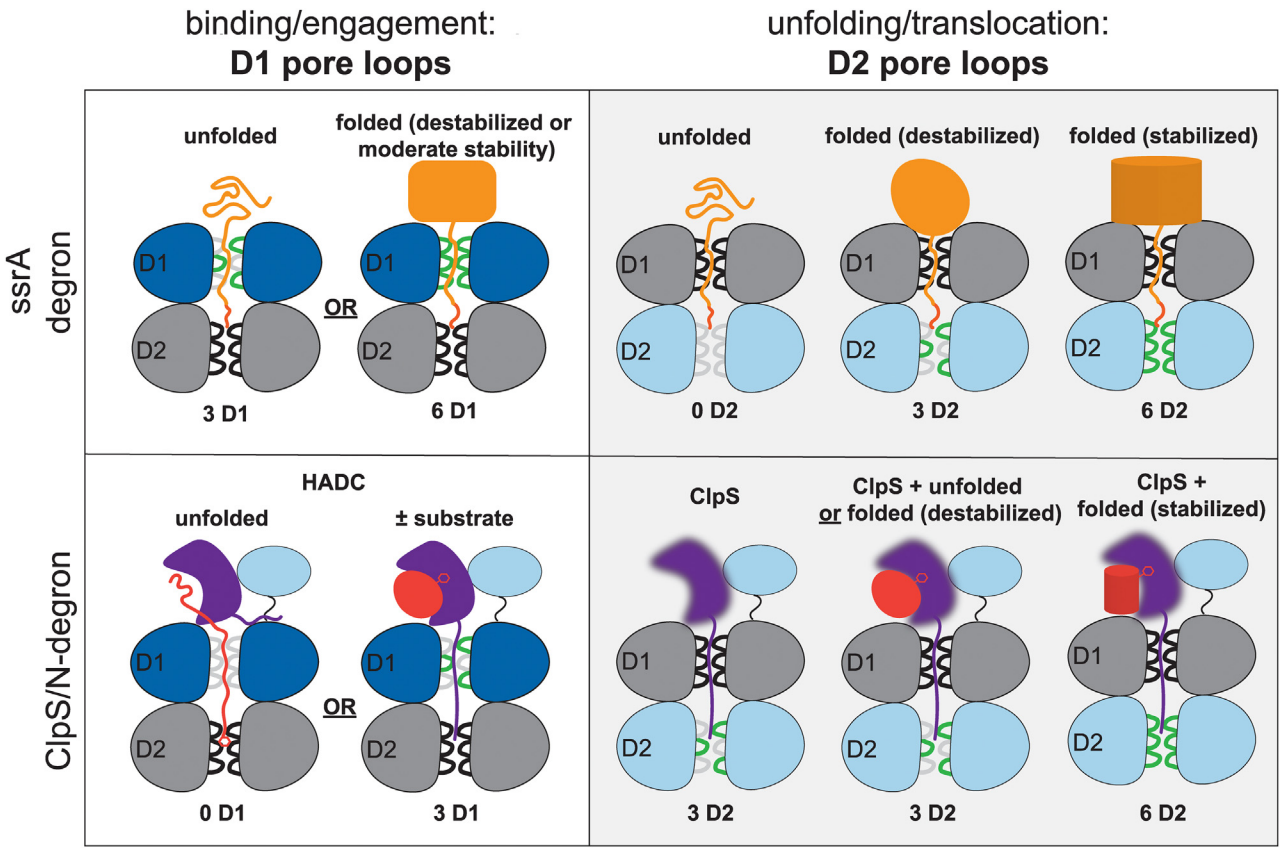

Figure 6. Summary of division of labor among D1 and D2 pore loops to coordinate substrate processing. Binding/engagement of direct degron substrates (*i.e.*, ssrA) and ClpS assisted degron substrates (*i.e.*, N-degron) requires different numbers of D1 pore loops. *Green pore loops* designate WT loops, whereas *light-gray loops* are defective. In all panels, *black loops* are not included in the analysis of pore loop function but included in the cartoons to illustrate complete ClpA•substrate complexes. *Top*, *left*, three or six WT D1 pore loops are required to bind/engage unfolded (*orange line*) or folded (*orange square*) ssrA-tagged substrates, respectively. *Bottom*, *left*, although an unfolded substrate (*red line*) can bypass the requirement for D1 pore loops for engagement and form an HADC with no WT D1 pore loops, three WT pore loops are generally required to form an HADC between ClpA, ClpS, and a folded substrate (*red oval*) or peptide. *Top*, *right*, unfolding and/or translocation by D2 pore loops requires different numbers of pore loops depending on the stability of the ssrA-tagged substrate: zero (unfolded, *orange line*), three (folded, destabilized, *orange oval*), or six (folded, stabilized, *orange cylinder*). *Bottom*, *right*, three WT D2 pore loops are required to "tug" and remodel ClpS before N-degron substrate delivery. The unfolding/translocation of N-degron substrates depends on the substrate stability properties: no additional pore loops are required to unfold/translocate unfolded or folded but destabilized substrates (*red oval*), suggesting that "tugging" on ClpS is the rate-limiting step. However, a folded substrate (*red cylinder*) requires six WT D2 pore loops. In this case, ClpS must first be "tugged" and remodeled as a prerequisite to ClpA unfolding/translocating the folded substrate. HADC, high-affinity delivery complex.

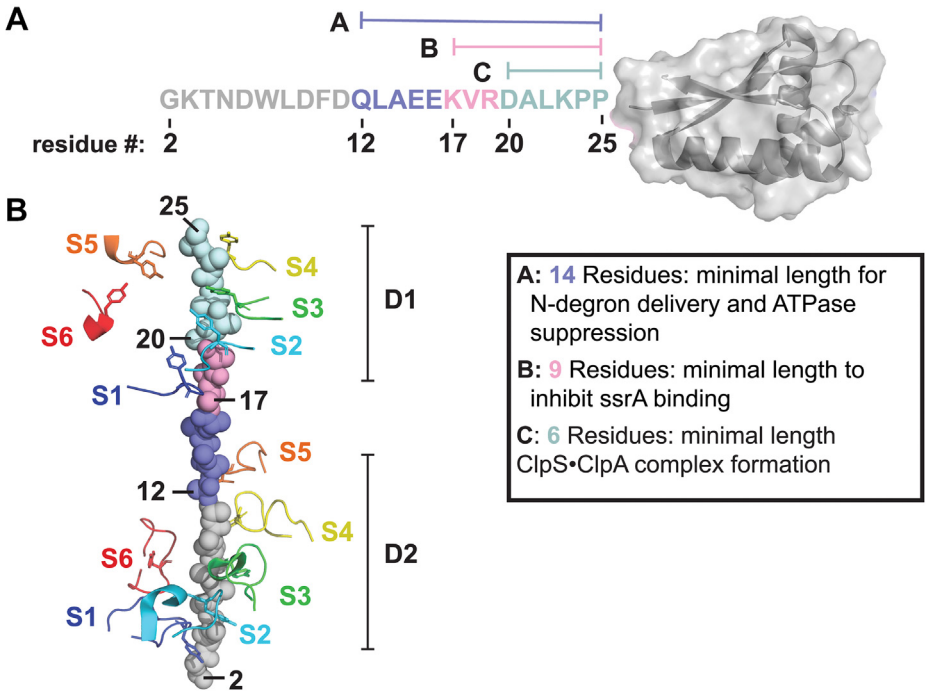

Figure 7. Model of ClpS•ClpA structure-function relationships. *A*, the NTE sequence (residues 2–25) and core domain (residues 26–106; PDB 3O2B) of ClpS with regions implicated in: (A) ClpS•ClpA complex formation in *teal*; (B) the ability of ClpS to inhibit ssrA-tag binding to ClpA in a noncompetitive fashion in *teal* + *pink*; and (C) the minimum length of the NTE need to promote N-degron delivery and inhibit ClpA's ATPase activity in *teal* + *pink* + *purple*. *B*, structure of a substrate polypeptide (modeled as polyalanine) engaged within the ClpA channel (PDB 6W1Z). Only the D1 pore-1 loops and the D2 pore-1 loops of the ClpA structure are shown for clarity (colored and labeled by subunits S1–S6). The substrate chain is color-coded as in panel *A* with ClpS residue numbers shown in *black*. NTE, N-terminal extension.

ClpS core domain (33), prolines in the NTE also appear to help ClpS resist ClpAP degradation. The susceptibility of $ClpS^{AA}$ to ClpAP degradation was not because of global destabilization of ClpS, as determined by the unchanged chemical denaturation profile of $ClpS^{AA}$ compared with ClpS (42). Therefore, although the mechanism is not yet known, we reason that changing the Pro^{24}-Pro^{25} sequence in ClpS to Ala-Ala alters the ClpA•ClpS interactions at the junction such that $ClpS^{AA}$ is degraded but WT ClpS is not. For example, perhaps the unique conformational constraints of a Pro-Pro dipeptide somehow disrupt ClpA's normal contacts with the polypeptide and thereby impede its function.

To investigate the difference between a Pro-Pro and an Ala-Ala sequence on ClpAP activity separately from the context of ClpS, we generated two model substrates; a Pro-Pro or Ala-Ala sequence was inserted between the ssrA degron and the stably folded native domain of GFP (43) (Fig. S2*B*). The Pro-Pro sequence inhibited the rate of ClpAP proteolysis of GFP-ssrA at least 10-fold compared with the Ala-Ala insertion (Fig. S2*B*). Because the Pro-Pro sequence alone can be transplanted to a model substrate and inhibit ClpAP degradation, similar to its effect in WT ClpS, we posit that $ClpS^{AA}$ degradation provides a useful, orthogonal readout for the action of ClpA's central pore loops when they interact with the ClpS NTE.

Therefore, to test the roles of the D2 pore loops in ClpA-promoted changes in ClpS structure, we monitored ClpAP degradation of the $ClpS^{AA}$ mutant. $ClpA^{xl}P$ degraded $ClpS^{AA}$ to completion in 30 min, whereas degradation by $^{D2\text{-}6A}ClpA^{xl}P$ was barely detectable (Fig. 5*C*), supporting our model that D2 pore loops normally "tug" on the ClpS NTE. With WT ClpS, this action could remodel the adapter and facilitate N-degron delivery whereas this "tugging" action successfully unfolds and translocates the $ClpS^{AA}$ variant resulting in its degradation. Interestingly, $^{D2\text{-}3YA}ClpA^{xl}P$ supported the degradation of $ClpS^{AA}$ at the same rate as $ClpA^{xl}P$, indicating that three WT D2 pore loops are as good as six in unfolding and then degrading $ClpS^{AA}$ (Fig. 5*C*). Moreover, $^{D2\text{-}3YA}ClpA^{xl}$, but not $^{D2\text{-}6A}ClpA^{xl}$, was also active in ClpS-dependent N-degron substrate delivery (see Fig. 4*B*, compare variants 4–5), establishing parallels between the degradation of $ClpS^{AA}$ and ClpS remodeling, which is required for successful substrate transfer to ClpAP. Together with the inability of $^{D2\text{-}6A}ClpA^{xl}$ to degrade ^{UF}YLFVQ-titin in the presence ClpS, but not in its absence (Fig. 4*B*), these results strongly suggest that active D2 pore loops of ClpA are required to remodel ClpS as a prelude to delivery of N-degron substrates to ClpP.

Discussion

Two AAA+ rings allow the division of labor between ClpA's D1 and D2 AAA+ modules

Sequence homology, mutagenesis studies, and their location lining the axial substrate-binding channel all indicate that the pore-1 loops are fundamental components of the inner workings of AAA+ unfoldases (15, 18, 19, 37, 44–47). Their precise functions, and how the work of the pore loops is divided between the two rings of double-ring enzymes, have

been difficult to dissect. Here, we use crosslinking to assemble pseudohexamers with WT or mutant pore-1 loops at specific positions and demonstrate unique functions for the D1 *versus* the D2 pore loops during the degradation process of both ssrA-tagged proteins and N-degron substrates delivered by the ClpS adapter (summarized in Fig. 6).

The ssrA degron is directly recognized within the ClpA channel, and a previous study which captured ClpA crosslinked to the ssrA tag indicated that initial complex formation likely occurs between the tag and D1 ring (15). Our present work, which compares the ability of ClpAP pore-loop variants to degrade a spectrum of ssrA-tagged substrates with different folding characteristics allows us to assign specific functions to the D1 and D2 pore loops (Fig. 6, *top*). When substrate unfolding is not needed, the D1 pore loops are necessary and sufficient for ssrA-tagged substrate degradation and can thus mediate substrate binding/engagement and translocation of the unfolded substrate into ClpP (Fig. 6, *top*; Fig. 3*A*). In the absence of WT D1 pore loops, the K_M for ^{UF}titin-ssrA degradation is >20-fold weaker than for ClpA variants with WT D1 pore loops (Fig. 3*B* and Table S1). In contrast, when unfolding of ssrA-tagged substrates is required, at least three WT D2 pore loops in addition to six D1 pore loops are necessary for degradation, indicating that unfolding requires unique contributions from the pore loops in the D2 ring (Fig. 6, right, *top*). Three WT D2 loops promote parental rates of unfolding of the destabilized titin^{V13P}-ssrA substrate, but six WT D2 loops mediate faster degradation of the more stable ^{cp7}GFP-ssrA protein (Fig. 3, *C* and *D*). These results suggest that the unfolding power contributed by these loops is at least partially additive. Taken together, our results with ssrA-tagged substrate degradation provide strong evidence that the D1 pore loops are critical for productive binding and engagement of the ssrA degron, whereas the D2 pore loops principally participate in the work of unfolding these substrates (Fig. 6, *top*).

Both the D1 and D2 pore loops of ClpA can promote substrate translocation. As noted above, a variant with only WT D1 loops translocates an unfolded ssrA-tagged substrate into ClpP for degradation (Fig. 3*A*). As the D2 loops perform unfolding, it is likely they can also perform the similar mechanical process of translocation. In support of this conclusion, a variant with only WT D2 loops supports efficient ClpAPS degradation of an unfolded N-degron substrate (Fig. 4*B*).

ClpA is a slightly slower translocase than the single-ring AAA+ ClpX enzyme (39). The redundant translocation activities of the two ClpA rings may contribute to slower translocation, as we find that mutating the D2 pore loops increases the rate of ClpAP degradation of the unfolded ssrA-tagged substrate (Fig. 3, *A* and *B*). The larger number of pore-loop contacts between WT ClpA and a substrate apparently slows translocation, whereas the additional substrate contacts from the combined D1 and D2 pore loops likely contribute to ClpA unfolding many substrates at faster rates than ClpX (39). The redundant ability of D1 and D2 pore loops to promote translocation also agrees well with the previous observation that the D1 motor antagonizes the stalling of ClpA (13). The fact that the D1 ring has independent translocation activity explains how it can function as a "back up" or "anti-stalling motor" for the more powerful D2 ring.

GYVG pore loops perform different jobs in ClpA and ClpX

The single AAA+ ring of ClpX and the D2 ring of ClpA are members of the same HCLR evolutionary clade of AAA+ modules and both have the conserved "GYVG" sequence motif in their pore-1 loops. In ClpX, these GYVG-family pore loops are key participants in the recognition of ssrA degrons, substrate grip, unfolding, and translocation (15, 17, 19, 37, 44–46), whereas our results reveal that ClpA has "outsourced" some of these functions to the D1 KYR loops. Biochemical comparison of the pore-1 loop mutant variants of ClpX and ClpA illustrate this difference. ClpX with no WT GYVG pore-1 loops is essentially inactive in degrading an unfolded ^{UF}titin-ssrA substrate, and ClpX with three WT pore-1 loops in an alternating arrangement only restores partial degradation activity, as K_M remains 20-fold weaker and V_{max} is 15-fold slower compared with WT ClpXP (37). In contrast, we find that $^{D2\text{-}6A}$ClpA^{xl}, with no WT GYVG D2 pore loops, and $^{D2\text{-}3YA}$ClpA^{xl}, with three alternating mutant and WT D2 pore loops, both support the degradation of ^{UF}titin-ssrA with V_{max} and K_M values very similar to the parental enzyme (Fig. 3*B* and Table S1). We also establish that in ClpA, the D1 KYR pore loops can perform substrate translocation and are critical for ssrA-engagement (Fig. 3, *A* and *B*). Hence, because ClpA has two rings, the GYVG D2 pore loops are not needed for recognition of ssrA-tagged substrates and their role in translocation can be shared with the KYR loops in the D1 ring. Having two AAA+ rings allows each ring to evolve more specialized functions and, importantly, enables ClpA to recognize/engage distinct substrates and substrate/adapter complexes.

N-degron delivery by ClpS requires both sets of ClpA pore loops

We find that the WT pore loops of both the D1 and D2 AAA+ rings participate in ClpS-mediated delivery of N-degron substrates (Fig. 6, *bottom*). For example, ClpA variants lacking six WT D1 or six WT D2 pore loops fail to degrade YLFVQELA-GFP, whereas three WT pore loops in either ring in combination with six WT pore loops in the other ring restore low levels of degradation of this substrate (Fig. 4*A*).

WT D1 pore loops function in stabilizing the ClpAP•ClpS•N-degron HADC complex and are required for ClpS to suppress the rate of ATP hydrolysis by ClpA in the presence of YLFVQELA-GFP or an N-degron peptide. However, D1 pore loops are not required for ClpS to suppress ClpA's ATPase activity in the presence of an unfolded N-degron substrate (Figs. 5*B* and 6, left, *bottom*). We propose that the requirement of the ClpA D1 pore loops for ClpAPS HADC complex stabilization may be partially bypassed in this case because the unfolded substrate substitutes in part for the role(s) of the ClpS NTE. For example, a long, unfolded

substrate (such as ^{UF}titin-ssrA which contains ~98 residues) may be able to both simultaneously bind to the ClpS core and enter the ClpA channel to make important contacts with the pore loops of the D2 ring, similar to those normally made by the NTE.

Unlike D1 pore loops, WT D2 pore loops play no detectable role in assembling ClpAP•ClpS•N-degron complexes or in forming the proper complexes to mediate suppression of ATP hydrolysis but are essential for ClpAPS degradation of native and unfolded N-degron substrates (Figs. 4–6). These results, together with previous studies, suggest that the engagement of and tugging on the ClpS-NTE by the WT D2 pore loops occurs after initial assembly of the ternary complex. By this scenario, the ClpA D2-pore loop•NTE interaction is required to remodel ClpS, triggering release of the N-degron substrate and its transfer to ClpAP for degradation (Fig. 6, right, *bottom*).

When comparing the pore-loop functions during degradation of ssrA-tagged *versus* N-degron substrates, a major emerging conclusion is that parallel elements and mechanisms are used by ClpA in both pathways. For example, during both types of degradation, the D2 pore loops perform critical unfolding/remodeling functions. However, there is an important distinction in the reaction sequences: although in both pathways the D2 ring must unfold any native structure within the substrate to allow its translocation into ClpP during N-degron degradation, the D2 ring must first forcefully remodel ClpS to free the substrate. Thus, although ClpS reprograms ClpAP to enable it to degrade two very distinct classes of substrates, this adapter-mediated regulatory mechanism incurs the additional energetic cost of ClpA remodeling ClpS.

Structural support for D1 and D2 pore loop functions during ClpS delivery

Our results reveal unique functional interactions between ClpS and the D1 and D2 pore-1 loops of ClpA. Previous biochemical analyses show that six NTE residues abutting the ClpS core domain (res. 20–25) are involved in ClpS•ClpA complex formation, nine residues (res. 17–25) mediate inhibition of ssrA-tagged substrate binding, and 14 residues (res. 12–25) are necessary for maximal inhibition of the ClpA ATPase and delivery of N-degron substrates (27, 28, 33, 34) (Fig. 7*A*). Because ClpA appears to use similar mechanisms to engage and "tug" on the NTE of ClpS as it does when attempting to unfold ssrA-tagged substrates, we were curious if the results from our study and previous biochemical data were consistent with the emerging structural evidence regarding substrate binding in the ClpA central channel. Importantly, the length, but not the sequence, of the ClpS NTE is critical for ClpS function (28). We modeled potential NTE interactions with ClpA pore loops by mapping three NTE segments (residues 20–25 in teal, 17–19 in pink, and 12–16 in purple) onto a 24-residue substrate peptide modeled as poly-alanine from a recent ClpA•substrate structure (14). In Figure 7*B*, the pore loops from D1 and D2 are each shown in rainbow colors from subunit one (indigo) to subunit six (red) (PDB 6W1Z) (14).

The modeled structure of the ClpS NTE in the ClpA channel agrees with numerous biochemical observations. For example, residues 20 to 25, which are required for strong ClpS•ClpA complex formation (33), correspond to an area (teal) on the substrate contacted by three D1 pore loops, consistent with our data that some, but not all, D1 pore loops are required to form this ClpS•ClpA complex (Fig. 7*B*). In addition, residues 17 to 25 (teal and pink), which represent the region of ClpS required for inhibition of ssrA-degron binding (27, 28), are in direct contact with the D1 pore loops. ClpS initially binds to the N-terminal domains of ClpA, and ssrA-tagged substrates bind directly in the ClpA channel. However, ClpS and ssrA-degrons may compete for ClpA D1 pore loops during productive engagement, a step following initial binding (27, 48). In fact, our biochemical data support the essential roles of D1 pore loops for engaging both ssrA degrons and ClpS, suggesting that ClpS inhibition of binding of ssrA-tagged substrates to ClpA could be, at least in part, a consequence of blocking access to the D1 pore loops. Lastly, the minimal length of the ClpS NTE required for N-degron delivery and maximal ATP suppression, 14 residues, (residues 12–25, teal, pink, and purple) spans D1 and is just long enough to contact the top pore loop in the D2 ring (subunit 5, orange) when mapped onto the poly-alanine substrate (Fig. 7*B*). This arrangement of the NTE within the ClpA channel is very attractive, as the proposed next step in N-degron substrate degradation is remodeling of the ClpS structure to transfer the substrate to the ClpA pore, a step that requires the pore loops and unfolding power of the D2 ring.

Is division of labor a common feature of double-ring unfoldases?

Do other double-ring unfoldases divide work between their two rings, as we see with ClpA? ClpC and ClpB are double-ring AAA+ unfoldases that share strong D1 and D2 pore-loop homology with D1 and D2 of ClpA (Fig. 1*A*) (17, 49, 50). Mutational analysis of the *Bacillus subtilis* MecA-ClpCP adapter-protease complex reveals that inactivating the D1 loops by Tyr to Ala substitutions eliminates the degradation of all substrates tested but mutating the D2 loops only reduces degradation rates (51). These results are consistent with the mechanism we propose for ClpAP, suggesting that the D1 pore loop mutations in ClpC hinder substrate binding and engagement, whereas D2 pore-loop mutations may slow, but not completely inactivate the enzyme's mechanical processes. Likewise, the D1 pore loops of *E. coli* ClpB are more important than its D2 loops for the enzyme's innate disaggregase activity in the absence of DnaK/DnaJ, once again consistent with the model that the pore loops of the D1 ring are critical for proper substrate engagement (52). In the presence of DnaK/DnaJ, however, the D2 pore loops become more critical for ClpB function (52), suggesting that these chaperones somehow function together with the D2 pore loops. Thus, ClpA, ClpB, and ClpC may all divide the jobs of their AAA+ rings and pore

loops in a similar manner, with the D1 loops principally engaging the substrate and the D2 loops focusing on the mechanical work of protein unfolding. Cdc48/p97/VCP (with "KMA" motifs in the pore 1 loops) is more sequence-divergent than ClpA, ClpB, and ClpC, but also conforms to a "division of labor" model. For example, the methionine of the D1 pore loop photo-crosslinks to substrate in the central channel, suggesting that these D1 pore loops are important for binding/engaging substrates (53). Furthermore, although the D1 pore loops have no observed roles in translocation, the D2 ("MWYG") pore loops participate in ATP-dependent substrate unfolding and translocation (53, 54). Thus, despite differences in unfoldase sequence/clade, biological function (disaggregase *versus* protease component), substrate specificity, and adapter usage, these double-ring unfoldases all display evidence of division of labor among the D1 and D2 pore loops that is reminiscent of the model we describe for ClpA. Especially clear is the emerging theme that the D1 pore loops play a critical role in substrate recognition and engagement.

Experimental procedures

Proteins and peptides

The QuikChange PCR technique (Agilent) was used to introduce crosslinking and pore-loop mutations into a pET23b (Novagen) containing *E. coli* His_7-SUMO-$ClpA^{\Delta C9,M169T,C47S,C203S,C243S}$ (His_7-SUMO is a solubility tag; the ΔC9 deletion prevents auto-degradation (35); M169T helps overexpression (55); and the C47S, C203S, and C243S mutations generate cysteine-free ClpA (12)). Plasmids encoding each ClpA variant fusion protein were transformed into *E. coli* strain BL21(DE3) and purified using cation-exchange and size-exclusion chromatography following cleavage of the His_7-SUMO fusion tag, as described (12). WT ClpA and ClpP were purified, as described (56). ClpS, $ClpS^{AA}$, YLFVQELA-GFP, and YLFVQ-$titin^{I27}$ were purified using established protocols from His_6-SUMO fusion protein constructs (33, 41, 57). Briefly, all proteins were purified by Ni-NTA and Superdex-75 size-exclusion chromatography (GE Healthcare) following Ulp1 cleavage of the His_6-SUMO fusion tags. ^{cp7}GFP-ssrA and $titin^{V13P}$-ssrA were purified, as described (38, 40). Pro-Pro and Ala-Ala mutants were introduced into pT7 GFP Gly12 ssrA (43) by round-the-horn PCR mutagenesis with T4 PNK and Q5 high-fidelity polymerase (New England Biolabs). GFP-PP-ssrA and GFP-AA-ssrA were expressed and purified, as described (43). For fluorescence assays, ^{UF}YLFVQ-$titin^{I27}$ and $^{UF}titin^{V13P}$-ssrA were labeled with 5-iodoacetamidofluorescein by an established protocol (37). LLYVQRDSKEC-amide and LLYVQRDSKEC-fl synthetic peptides were purchased from 21st Century Biochemicals. The synthetic RseA peptide was synthesized by standard FMOC techniques using an Apex 396 solid-phase instrument.

Crosslinking

^{D645C}ClpA and ^{Q709C}ClpA variants were purified from cysteine-free ClpA backgrounds containing WT or defective pore-1 loops (Y259A or Y540A) and were exchanged from Activity Buffer (50 mM HEPES-KOH pH 7.5, 20 mM $MgCl_2$, 0.3 M NaCl, 10% (v/v) glycerol, and 2 mM tris(2-carboxyethyl) phosphine (TCEP)) into Crosslinking Buffer (50 mM HEPES-KOH pH 7, 300 mM NaCl, 20 mM $MgCl_2$, 10% glycerol, and 5 mM EDTA) using Zeba Spin Desalting Columns (ThermoFisher Scientific). Crosslinking was carried out in the crosslinking buffer, as described (12). Briefly, the reactions containing ClpA variants and a homobifunctional crosslinker (1,4-bismaleimidobutane; ThermoFisher Scientific) were incubated for ∼30 min at room temperature before quenching by the addition of 50 mM DTT. The crosslinked ClpA dimers were then separated from monomers by chromatography on a Superdex 200 16/600 size-exclusion column (GE Healthcare) in the Activity buffer. The absence of ATP or ATPγS in the Activity buffer prevents the stable ClpA hexamer assembly during chromatography. The fractions containing crosslinked dimers were flash frozen and stored at −80 °C.

Pore-opening assay

ClpP cleavage of a fluorogenic RseA decapeptide (Abz-KASPVSLGY^{NO2}D; 15 μM) was assayed in the Activity Buffer in the presence of ATPγS (2 mM) and different ClpA variants (0.50 μM), and ClpP (0.25 μM) (36). Abz is a 2-aminobenzoic acid fluorophore, and Y^{NO2} is a 3-nitrotyrosine quencher. The rate of peptide degradation was monitored by fluorescence (excitation 320 nm; emission 420 nm) using a SpectraMax M5 Microplate Reader (Molecular Devices).

ATP-hydrolysis assays

ATPase assays were performed at 30 °C in the Activity Buffer containing $ClpA_6$ variants (0.1 μM), $ClpP_{14}$ (0.3 μM), plus or minus ClpS (0.1 μM when present). The hydrolysis of 5 mM ATP (Sigma-Aldrich) was measured using an NADH-coupled assay (56) with an ATP-regeneration system (20 U/ml pyruvate kinase, 20 U/ml lactate dehydrogenase, 7.5 mM phosphoenolpyruvate, and 0.2 mM NADH) by monitoring the loss of absorbance at 340 nm using a SpectraMax Plus 384 Microplate Reader (Molecular Devices).

Degradation assays

Degradation was assayed in the Activity Buffer at 30 °C. To monitor ClpAP degradation of YLFVQELA-GFP (1 μM), ^{UF}YLFVQ-titin (1 μM), or ^{UF}titin-ssrA (0.3125–20 μM), the reactions contained $ClpA_6$ (0.1 μM), $ClpP_{14}$ (0.3 μM), plus or minus ClpS (0.1 μM), ATP (4 mM), and an ATP-regeneration system (6.25 mM phosphoenolpyruvate and 23.5 U/ml pyruvate kinase). The degradation of ^{cp7}GFP-ssrA (10 μM) was assayed using $ClpA_6$ (0.3 μM), $ClpP_{14}$ (0.8 μM), ATP (4 mM), and the ATP-regeneration system. The degradation of GFP-AA-ssrA or GFP-PP-ssrA (8 μM) was assayed using $ClpA_6$ (0.25 μM), $ClpP_{14}$ (0.75 μM), ATP (5 mM), and the ATP-regeneration system. The loss of GFP fluorescence (excitation 467 nm; emission 511 nm) or increase in ^{UF}titin fluorescence (excitation 495 nm; emission 518 nm) was monitored using a SpectraMax M5 Microplate Reader. The

degradation of ^{UF}titin was quantified by normalizing the relative fluorescence units to the total ^{UF}titin degraded upon the addition of porcine elastase (0.1 mg/ml; Sigma-Aldrich) for 30 min at the end of the assay.

To assay the degradation of titin^{V13P}-ssrA or ClpS^{AA} by ClpAP variants, $ClpA_6$ (0.25 μM), $ClpP_{14}$ (0.75 μM), ATP (5 mM), and the ATP-regeneration system were preincubated at 30 °C for 2 min, and either titin^{V13P}-ssrA (10 μM) or ClpS^{AA} (5 μM) was added to initiate degradation. The samples were taken at different time points, quenched by the addition of SDS-sample buffer and rapid freezing, and later thawed, boiled, and electrophoresed on a Mini-PROTEAN TGX 4 to 20% (weight/volume) precast gel (Bio-Rad). The bands were visualized by staining with SYPRO Red protein stain (ThermoFisher) and quantified using a Typhoon FLA 9500 scanner (GE Healthcare) and with ImageQuant 8.1 software (GE Healthcare). For both the gels, the fraction of substrate remaining was calculated by dividing the density of the substrate band at each time point by the density at time zero, after normalization of the amount of the sample in each lane using the ClpP density.

Fluorescence anisotropy assays

Binding assays monitored by fluorescence anisotropy of LLYVQRDSKEC-fl (100 nM) were performed using a SpectraMax M5 Microplate Reader at 30 °C in the Activity Buffer. ATPγS (2 mM), ATP (10 mM), and ClpP (1 μM) were used where designated. ClpA and ClpS were used in a 1:1 ratio, with concentrations varying from 0.1 to 1 μM. The data (n ≥ 3 ± 1 SD) were fitted to the quadratic form of the binding equation appropriate for tight binding. The K_{app} values are reported with average errors (typically 4–5%).

Data availability

All data are contained in the article or supporting information.

Supporting information—This article contains supporting information.

Acknowledgments—We thank I. Levchenko (MIT) for materials and X. Fei (MIT) for helpful insight into ClpA-ClpS structural features, J. Zhang (MIT) for critical reading of the article, and other members of our labs for experimental advice and suggestions.

Author contributions—K. L. Z., S. K., R. T. S., and T. A. B. conceptualization; K. L. Z., S. K., R. T. S., and T. A. B. methodology; K. L. Z., R. T. S., and T. A. B. project administration; K. L. Z. and S. K. investigation; K. L. Z., S. K., R. T. S., and T. A. B. formal analysis; K. L. Z., S. K., R. T. S., and T. A. B. validation; K. L. Z. visualization; K. L. Z. and T. A. B. writing–original draft; K. L. Z., S. K., R. T. S., and T. A. B. writing–reviewing and editing; K. L. Z. and S. K. resources; R. T. S. and T. A. B. supervision; K. L. Z., S. K., R. T. S., and T. A. B. funding acquisition.

Funding and additional information—This work was supported by NIH grant AI-016892 (R. T. S. and T. A. B.), the Howard Hughes Medical Institute (T. A. B.), and the National Science Foundation Graduate Research Fellowships under Grant no. 1745302 (to K. L. Z. and S. K.). The content is solely the responsibility of the authors and does not necessarily represent the official views of the National Institutes of Health.

Conflict of interest—The authors declare that they have no conflicts of interest with the contents of this article.

Abbreviations—The abbreviations used are: AAA+, ATPases associated with diverse cellular activities; HADC, high-affinity delivery complex; NTE, N-terminal extension.

References

1. Snider, J., Thibault, G., and Houry, W. A. (2008) The AAA+ superfamily of functionally diverse proteins. *Genome Biol.* **9**, 216
2. Hanson, P. I., and Whiteheart, S. W. (2005) AAA+ proteins: Have engine, will work. *Nat. Rev. Mol. Cell Biol.* **6**, 519–529
3. Neuwald, A. F., Aravind, L., Spouge, J. L., and Koonin, E. V. (1999) AAA+: A class of chaperone-like ATPases associated with the assembly, operation, and disassembly of protein complexes. *Genome Res.* **9**, 27–43
4. Sauer, R. T., Bolon, D. N., Burton, B. M., Burton, R. E., Flynn, J. M., Grant, R. A., Hersch, G. L., Joshi, S. A., Kenniston, J. A., Levchenko, I., Neher, S. B., Oakes, E. S. C., Siddiqui, S. M., Wah, D. A., and Baker, T. A. (2004) Sculpting the proteome with AAA+ proteases and disassembly machines. *Cell* **119**, 9–18
5. Sauer, R. T., and Baker, T. A. (2011) AAA+ proteases: ATP-fueled machines of protein destruction. *Annu. Rev. Biochem.* **80**, 587–612
6. Katayama, Y., Gottesman, S., Pumphrey, J., Rudikoff, S., Clark, W. P., and Maurizi, M. R. (1988) The two-component, ATP-dependent Clp protease of *Escherichia coli*. Purification, cloning, and mutational analysis of the ATP-binding component. *J. Biol. Chem.* **263**, 15226–15236
7. Hwang, B. J., Woo, K. M., Goldberg, A. L., and Chung, C. H. (1988) Protease Ti, a new ATP-dependent protease in *Escherichia coli*, contains protein-activated ATPase and proteolytic functions in distinct subunits. *J. Biol. Chem.* **263**, 8727–8734
8. Schmidt, R., Zahn, R., Bukau, B., and Mogk, A. (2009) ClpS is the recognition component for *Escherichia coli* substrates of the N-end rule degradation pathway. *Mol. Microbiol.* **72**, 506–517
9. Erbse, A., Schmidt, R., Bornemann, T., Schneider-Mergener, J., Mogk, A., Zahn, R., Dougan, D. A., and Bukau, B. (2006) ClpS is an essential component of the N-end rule pathway in *Escherichia coli*. *Nature* **439**, 753–756
10. Tobias, J. W., Shrader, T. E., Rocap, G., and Varshavsky, A. (1991) The N-end rule in bacteria. *Science* **254**, 1374–1377
11. Kress, W., Mutschler, H., and Weber-Ban, E. (2009) Both ATPase domains of ClpA are critical for processing of stable protein structures. *J. Biol. Chem.* **284**, 31441–31452
12. Zuromski, K. L., Sauer, R. T., and Baker, T. A. (2020) Modular and coordinated activity of AAA+ active sites in the double-ring ClpA unfoldase of the ClpAP protease. *Proc. Natl. Acad. Sci. U. S. A.* **117**, 25455–25463
13. Kotamarthi, H. C., Sauer, R. T., and Baker, T. A. (2020) The non-dominant AAA + ring in the ClpAP protease functions as an anti-stalling motor to accelerate protein unfolding and translocation. *Cell Rep.* **30**, 2644–2654
14. Lopez, K. E., Rizo, A. N., Tse, E., Lin, J., Scull, N. W., Thwin, A. C., Lucius, A. L., Shorter, J., and Southworth, D. R. (2020) Conformational plasticity of the ClpAP AAA+ protease couples protein unfolding and proteolysis. *Nat. Struct. Mol. Biol.* **27**, 406–416
15. Hinnerwisch, J., Fenton, W. A., Furtak, K. J., Farr, G. W., and Horwich, A. L. (2005) Loops in the central channel of ClpA chaperone mediate protein binding, unfolding, and translocation. *Cell* **121**, 1029–1041
16. Guo, F., Maurizi, M. R., Esser, L., and Xia, D. (2002) Crystal structure of ClpA, an Hsp100 chaperone and regulator of ClpAP protease. *J. Biol. Chem.* **277**, 46743–46752

17. Schlieker, C., Weibezahn, J., Patzelt, H., Tessarz, P., Strub, C., Zeth, K., Erbse, A., Schneider-Mergener, J., Chin, J. W., Schultz, P. G., Bukau, B., and Mogk, A. (2004) Substrate recognition by the AAA+ chaperone ClpB. *Nat. Struct. Mol. Biol.* **11**, 607–615
18. Yamada-Inagawa, T., Okuno, T., Karata, K., Yamanaka, K., and Ogura, T. (2003) Conserved pore residues in the AAA protease FtsH are important for proteolysis and its coupling to ATP hydrolysis. *J. Biol. Chem.* **278**, 50182–50187
19. Siddiqui, S. M., Sauer, R. T., and Baker, T. A. (2004) Role of the processing pore of the ClpX AAA+ ATPase in the recognition and engagement of specific protein substrates. *Genes Dev.* **18**, 369–374
20. Farbman, M. E., Gershenson, A., and Licht, S. (2008) Role of a conserved pore residue in the formation of a prehydrolytic high substrate affinity state in the AAA+ chaperone ClpA. *Biochemistry* **47**, 13497–13505
21. Erbse, A. H., Wagner, J. N., Truscott, K. N., Spall, S. K., Kirstein, J., Zeth, K., Turgay, K., Mogk, A., Bukau, B., and Dougan, D. A. (2008) Conserved residues in the N-domain of the AAA+ chaperone ClpA regulate substrate recognition and unfolding. *FEBS J.* **275**, 1400–1410
22. Karzai, A. W., Roche, E. D., and Sauer, R. T. (2000) The SsrA-SmpB system for protein tagging, directed degradation and ribosome rescue. *Nat. Struct. Biol.* **7**, 449–455
23. Janssen, B. D., and Hayes, C. S. (2012) The tmRNA ribosome-rescue system. *Adv. Protein Chem. Struct. Biol.* **86**, 151–191
24. Dulebohn, D., Choy, J., Sundermeier, T., Okan, N., and Karzai, A. W. (2007) Trans-translation: The tmRNA-mediated surveillance mechanism for ribosome rescue, directed protein degradation, and nonstop mRNA decay. *Biochemistry* **46**, 4681–4693
25. Gottesman, S., Roche, E., Zhou, Y. N., and Sauer, R. T. (1998) The ClpXP and ClpAP proteases degrade proteins with carboxy-terminal peptide tails added by the SsrA-tagging system. *Genes Dev.* **12**, 1338–1347
26. Olivares, A. O., Baker, T. A., and Sauer, R. T. (2016) Mechanistic insights into bacterial AAA+ proteases and protein-remodelling machines. *Nat. Rev. Microbiol.* **14**, 33–44
27. Torres-Delgado, A., Kotamarthi, H. C., Sauer, R. T., and Baker, T. A. (2020) The intrinsically disordered N-terminal extension of the ClpS adaptor reprograms its partner AAA+ ClpAP protease. *J. Mol. Biol.* **432**, 4908–4921
28. Hou, J. Y., Sauer, R. T., and Baker, T. A. (2008) Distinct structural elements of the adaptor ClpS are required for regulating degradation by ClpAP. *Nat. Struct. Mol. Biol.* **15**, 288–294
29. Dougan, D. A., Reid, B. G., Horwich, A. L., and Bukau, B. (2002) ClpS, a substrate modulator of the ClpAP machine. *Mol. Cell* **9**, 673–683
30. Mogk, A., Schmidt, R., and Bukau, B. (2007) The N-end rule pathway for regulated proteolysis: Prokaryotic and eukaryotic strategies. *Trends Cell Biol.* **17**, 165–172
31. Zeth, K., Ravelli, R. B., Paal, K., Cusack, S., Bukau, B., and Dougan, D. A. (2002) Structural analysis of the adaptor protein ClpS in complex with the N-terminal domain of ClpA. *Nat. Struct. Biol.* **9**, 906–911
32. Guo, F., Esser, L., Singh, S. K., Maurizi, M. R., and Xia, D. (2002) Crystal structure of the heterodimeric complex of the adaptor, ClpS, with the N-domain of the AAA+ chaperone, ClpA. *J. Biol. Chem.* **277**, 46753–46762
33. Román-Hernández, G., Hou, J. Y., Grant, R. A., Sauer, R. T., and Baker, T. A. (2011) The ClpS adaptor mediates staged delivery of N-end rule substrates to the AAA+ ClpAP protease. *Mol. Cell* **43**, 217–228
34. Rivera-Rivera, I., Román-Hernández, G., Sauer, R. T., and Baker, T. A. (2014) Remodeling of a delivery complex allows ClpS-mediated degradation of N-degron substrates. *Proc. Natl. Acad. Sci. U. S. A.* **111**, E3853–E3859
35. Maglica, Ž., Striebel, F., and Weber-Ban, E. (2008) An intrinsic degradation tag on the ClpA C-terminus regulates the balance of ClpAP complexes with different substrate specificity. *J. Mol. Biol.* **384**, 503–511
36. Lee, M. E., Baker, T. A., and Sauer, R. T. (2010) Control of substrate gating and translocation into ClpP by channel residues and ClpX binding. *J. Mol. Biol.* **399**, 707–718
37. Iosefson, O., Nager, A. R., Baker, T. A., and Sauer, R. T. (2015) Coordinated gripping of substrate by subunits of a AAA+ proteolytic machine. *Nat. Chem. Biol.* **11**, 201–206
38. Kenniston, J. A., Baker, T. A., Fernandez, J. M., and Sauer, R. T. (2003) Linkage between ATP consumption and mechanical unfolding during the protein processing reactions of an AAA+ degradation machine. *Cell* **114**, 511–520
39. Olivares, A. O., Nager, A. R., Iosefson, O., Sauer, R. T., and Baker, T. A. (2014) Mechanochemical basis of protein degradation by a double-ring AAA+ machine. *Nat. Struct. Mol. Biol.* **21**, 871–875
40. Nager, A. R., Baker, T. A., and Sauer, R. T. (2011) Stepwise unfolding of a β barrel protein by the AAA+ ClpXP protease. *J. Mol. Biol.* **413**, 4–16
41. Wang, K. H., Sauer, R. T., and Baker, T. A. (2007) ClpS modulates but is not essential for bacterial N-end rule degradation. *Genes Dev.* **21**, 403–408
42. Rivera-Rivera, I. (2015) *Mechanism of Active Substrate Delivery by the AAA+ Protease Adaptor ClpS*. Ph.D. thesis, Massachusetts Institute of Technology
43. Bell, T. A., Baker, T. A., and Sauer, R. T. (2019) Interactions between a subset of substrate side chains and AAA+ motor pore loops determine grip during protein unfolding. *Elife* **8**, e46808
44. Martin, A., Baker, T. A., and Sauer, R. T. (2008) Diverse pore loops of the AAA+ ClpX machine mediate unassisted and adaptor-dependent recognition of ssrA-tagged substrates. *Mol. Cell* **29**, 441–450
45. Martin, A., Baker, T. A., and Sauer, R. T. (2008) Pore loops of the AAA+ ClpX machine grip substrates to drive translocation and unfolding. *Nat. Struct. Mol. Biol.* **15**, 1147–1151
46. Lum, R., Tkach, J. M., Vierling, E., and Glover, J. R. (2004) Evidence for an unfolding/threading mechanism for protein disaggregation by *Saccharomyces cerevisiae* Hsp104. *J. Biol. Chem.* **279**, 29139–29146
47. Weibezahn, J., Tessarz, P., Schlieker, C., Zahn, R., Maglica, Z., Lee, S., Zentgraf, H., Weber-ban, E. U., Dougan, D. A., Tsai, F. T. F., Mogk, A., and Bukau, B. (2004) Thermotolerance requires refolding of aggregated proteins by substrate translocation through the central pore of ClpB. *Cell* **119**, 653–665
48. Saunders, R. A., Stinson, B. M., Baker, T. A., and Sauer, R. T. (2020) Multistep substrate binding and engagement by the AAA+ ClpXP protease. *Proc. Natl. Acad. Sci. U. S. A.* **117**, 28005–28013
49. Miller, J. M., and Enemark, E. J. (2016) Fundamental characteristics of AAA+ protein family structure and function. *Archaea* **2016**, 9294307
50. Liu, J., Mei, Z., Li, N., Qi, Y., Xu, Y., Shi, Y., Wang, F., Lei, J., and Gao, N. (2013) Structural dynamics of the MecA-ClpC complex: A type II AAA+ protein unfolding machine. *J. Biol. Chem.* **288**, 17597–17608
51. Wang, F., Mei, Z., Qi, Y., Yan, C., Hu, Q., Wang, J., and Shi, Y. (2011) Structure and mechanism of the hexameric MecA-ClpC molecular machine. *Nature* **471**, 331–337
52. Doyle, S. M., Hoskins, J. R., and Wickner, S. (2012) DnaK chaperone-dependent disaggregation by caseinolytic peptidase B (ClpB) mutants reveals functional overlap in the N-terminal domain and nucleotide-binding domain-1 pore tyrosine. *J. Biol. Chem.* **287**, 28470–28479
53. Bodnar, N. O., and Rapoport, T. A. (2017) Molecular mechanism of substrate processing by the Cdc48 ATPase complex. *Cell* **169**, 722–735.e9
54. Rapoport, T., and Bodnar, N. (2017) Toward an understanding of the Cdc48/p97 ATPase. *F1000Res.* **6**, 1–10
55. Seol, J. H., Yoo, S. J., Kim, K. I., Kang, M. S., Ha, D. B., and Chung, C. H. (1994) The 65-kDa protein derived from the internal translational initiation site of the *clpA* gene inhibits the ATP-dependent protease Ti in *Escherichia coli*. *J. Biol. Chem.* **269**, 29468–29473
56. Kim, Y. I., Levchenko, I., Fraczkowska, K., Woodruff, R. V., Sauer, R. T., and Baker, T. A. (2001) Molecular determinants of complex formation between Clp/Hsp 100 ATPases and the ClpP peptidase. *Nat. Struct. Biol.* **8**, 230–233
57. Wang, K. H., Oakes, E. S. C., Sauer, R. T., and Baker, T. A. (2008) Tuning the strength of a bacterial N-end rule degradation signal. *J. Biol. Chem.* **283**, 24600–24607